Journal of Power Sources 215 (2012) 164–169

Contents lists available at SciVerse ScienceDirect

Journal of Power Sources

journal homepage: www.elsevier.com/locate/jpowsour

Flexible, metal-free composite counter electrodes for efficient fiber-shaped dye-sensitized solar cells

Shaocong Hou, Xin Cai, Hongwei Wu, Zhibin Lv, Dan Wang, Yongping Fu, Dechun Zou*

Beijing National Laboratory for Molecular Sciences, Key Laboratory of Polymer Chemistry and Physics of Ministry of Education, College of Chemistry and Molecular Engineering, Peking University, Beijing 100871, China

HIGHLIGHTS

- Flexible metal-free electrodes with core/shell structure were fabricated.
- Their electrochemical performances were systematically investigated.
- Fiber-shaped dye-sensitized solar cells were fabricated with fibrous electrodes.
- The amount of PEDOT:PSS and the diameters of the electrodes were optimized.

GRAPHICAL ABSTRACT

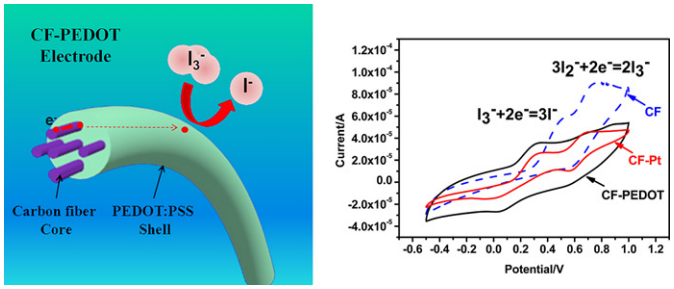

ARTICLE INFO

Article history:
Received 2 February 2012
Received in revised form
26 April 2012
Accepted 2 May 2012
Available online 18 May 2012

Keywords:
Carbon fibers
Conducting polymers
Counter electrodes
Dye-sensitized solar cells
Flexible electronics

ABSTRACT

Highly flexible metal-free fibrous electrodes are prepared using commercial carbon fiber (CF) and poly(3,4-ethylene dioxythiophene)-polystyrene sulfonate (PEDOT:PSS) aqueous solution. Multiple highly ordered CF monofilaments act as the conductive cores, while the PEDOT:PSS films act as the catalytic shell in the composite fibrous electrode. Cyclic voltammetry and electrochemical impedance spectroscopy are carried out to systematically investigate the electrochemical performance, and the results indicate that the composite fibrous electrode is highly efficient in catalyzing I_3^-/I^-. The PEDOT:PSS conductive films also show excellent compatibility with CF and resistance to solvent. The low-cost composite electrodes are used as counter electrodes to fabricate fiber-shaped dye-sensitized solar cells, and the highest conversion efficiency of 5.5% is achieved, which is comparable to the performance of platinized CF counter electrode-based device.

1. Introduction

Dye-sensitized solar cells (DSSCs) show great potential in solving energy and environmental crises, because they are cost-efficient and environmentally friendly [1]. DSSCs are based on the photoelectrochemical principle, and they are usually composed of the dye-sensitized TiO_2 nanocrystal photoanode, electrolyte-containing I_3^-/I^- redox species and a catalytic Pt counter electrode (CE). The photoelectrons generated *via* dye excitation upon illumination are immediately injected into the TiO_2 semiconductor, and the dyes are oxidized to dye^+. The electrons then transport through the photoanode and the outer circuit, and then reach the CE. Subsequently, the I_3^- species in the electrolyte are reduced to I^- species, which will then reduce the dye^+ to facilitate dye regeneration. Considering the functions of the CEs, they should have both excellent conductivity and catalytic ability toward I_3^-/I^- species [2,3]. Meanwhile, metallic Pt meets these two requirements, and thus is often preferred as the CE for DSSCs. However, Pt

* Corresponding author. Tel./fax: +86 10 6275 9799.
E-mail address: dczou@pku.edu.cn (D. Zou).

0378-7753/$ – see front matter © 2012 Elsevier B.V. All rights reserved.
doi:10.1016/j.jpowsour.2012.05.002

is scarce, expensive, and is easily corroded by iodine-based electrolytes. Moreover, high vacuum and high temperature caused by magnetron sputtering and thermal decomposition processes for preparing Pt films also bring additional costs, which are adverse for mass production. These problems have urged many researchers to explore new materials to replace Pt. The first category is low-cost carbon materials, including graphite [4], carbon black [5], porous carbon [6], powdered carbon fiber [7], carbon nanotubes [8], and graphene [9,10]. Carbon catalysts are usually milled into powders with high specific surface area to improve their catalytic activity, and then they are processed into thick porous films with organic or inorganic binders, resulting in electrolyte transport limitation and poor stability [11]. The second category is inorganic metal compounds, such as nitrides [12], carbides [13], sulfides [14], and oxides [15] of Ti, W, Co, and other metals, which also suffer from low catalytic activity and conductivity. The third category is conductive polymers, such as polyaniline [16–18], polypyrrole [19,20], and polythiophene derivatives [21–24], which show good catalytic performance to I_3^-/I^-, and thus they are potential substitutes for Pt. Among these conductive polymers, poly(3,4-ethylene dioxythiophene) (PEDOT) has drawn much attention because of its good catalytic performance, high conductivity and stability, as well as easy preparation. *In situ* polymerization [21,22], electrochemical polymerization [23,24], or direct coating of commercial PEDOT solution onto fluorine-doped tin oxide (FTO) glasses are conducted to obtain PEDOT-based CEs. However, the small catalytic area and poor adhesion of PEDOT to FTO substrates limit the fill factor and the conversion efficiency of PEDOT CE-based DSSCs. Some studies have shown that increasing the surface area of PEDOT electrode *via* the addition of carbon [25–27] or TiO_2 nanoparticles [28,29] could improve the device performance.

The indispensable and expensive transparent conductive oxides (TCOs) materials, such as indium tin oxide (ITO) and FTO, which are used as electrode substrates of typical DSSCs, are supposed to be limiting factors of the commercial application of DSSCs. Meanwhile, preparing high quality TCOs with both good conductivity and transparency is very difficult. Recently, TCO-free fiber-shaped DSSCs have been developed, and the electrode substrate has been expanded to highly conductive and opaque metal wires [30–34]. The conversion efficiency of a fiber-shaped DSSC with a Pt wire as the CE has attained above 7% [35]. Furthermore, fiber-shaped DSSC with commercial carbon fibers (CF) modified with Pt as CE reached an efficiency of 5%, and the amount of platinum utilized was less than 1% than that of the Pt wire [36]. Industrial CFs are abundant, light weight, flexible, and chemically stable. Moreover, long-ordered CF can be used directly without any binders, which are always used in nanocarbon-based CEs.

In the current study, flexible metal-free fibrous electrodes, that is, CF/PEDOT composite electrodes, are first prepared through a simple solution process which totally eliminate the use of high temperature and high vacuum. The systematic electrochemical analysis confirmed that CF/PEDOT electrodes have better catalytic performance and better stability than platinized CF (CF/Pt). Thus, the CF/PEDOT CE-based fiber-shaped solar cells showed conversion efficiency of up to 5.6%.

2. Experimental

2.1. Fabrication of CF/PEDOT and CF/Pt electrodes

Poly(3,4-ethylene dioxythiophene):poly(styrene sulfonate) aqueous solution (PEDOT:PSS, CLEVIOS PH 1000, purchased from Heraeus Ltd., Germany) was mixed with 5 wt% dimethyl sulphoxide (DMSO). Unless specified otherwise, the reagents were purchased from Sinopharm Chemical Reagent Beijing Co., Ltd. Carbon fiber yarns (M40J, purchased from Toray Industries Inc., Japan) were cut into short lengths (about 2 cm) and different diameters (φ = 50, 100, or 150 μm), and then washed with acetone. They were dipped into above mixed solution, pulled out, and then dried at 120 °C in air. The process was repeated until the desired number of dip-coating was attained (0, 2, 4, or 7 times). After drying for another 0.5 h, the CF/PEDOT electrodes were obtained. For the sake of comparison, a cleaned carbon fiber yarn (φ = 100 μm) was soaked in 5.0 mg ml^{-1} chloroplatinic acid aqueous solution, taken out, and then thermally decomposed for 20 min at 400 °C to obtain the CF/Pt electrode.

2.2. Fabrication of fiber-shaped DSSCs

Photoanodes were fabricated on Ti wires (φ = 250 μm, purchased from Alfa Aesar) *via* the dip-coating method described earlier, annealed, and sensitized with *Di-tetrabutylammonium cis-bis(isothiocyanato)bis(2,2′-bipyridyl-4,4′-dicarboxylato)ruthenium(II)* (dye N719) [36]. The acetonitrile-based electrolyte contained 0.03 M iodine, 0.5 M 1-butyl-3-methylimidazolium iodide, 0.3 M tert-butyl pyridine, 0.05 M lithium perchlorate, and 0.05 M guanidine thiocyanate. To obtain a final fiber-shaped DSSC, the CE was close to the photoanode in parallel, and then the two electrodes were simultaneously inserted into a glass capillary (Φ_{inner} = 0.9 mm, Φ_{outer} = 1.2 mm), then the electrolyte was filled into the capillary, Finally, the ends of the capillary were sealed with paraffin wax. The lengths of the fiber-shaped DSSCs were prepared to be 2 cm in length.

2.3. Characterization

The morphology of the CF/PEDOT electrode was observed using field-emission SEM (S-4800 Hitachi, Japan). Cyclic voltammetry (CV) of CF, CF/PEDOT, and CF/Pt electrodes were performed using a CHI electrochemical station (Shanghai Chenhua, China) in the electrolyte (3 mM iodine, 50 mM 1-butyl-3-methylimidazolium iodide, and 0.1 M lithium perchlorate) with an Ag/AgCl electrode as the reference electrode and Pt wire as the CE. *I–V* tests were conducted with an Advantest R6489 Source and a Keithley Multimeter 2000 under simulated light of AM 1.5G and 100 mW cm^{-2} (Sunlight Yamashita DESO). An AUTOLAB PG320 (Swiss) was used to measure the electrochemical impedance of the device between 1 MHz and 50 mHZ under dark conditions with a 0.7 V forward bias.

3. Results and discussion

3.1. Morphology of the CF/PEDOT electrodes

The CF/PEDOT electrodes were prepared *via* a simple dip-coating method with commercial CF and PEDOT:PSS solution. The PEDOT:PSS solution was doped with 5 wt% DMSO to improve the conductivity of the PEDOT conductive polymer [37]. The CF/PEDOT fibrous electrode preserves good flexibility that mainly originates from the flexible CF substrate and PEDOT polymer film, and thus it can be wrapped along a Ti wire-based photoanode (Fig. 1a). Fig. 1b shows the thin but robust PEDOT film coating on the CF. The good adhesion between the PEDOT and the CF favors the ohmic contact at their interfaces. The cross-sectional image (Fig. 1c) shows the multiple core–shell structure of the CF/PEDOT electrode. Each single CF monofilament was covered with a nanometer-thick PEDOT film, and some PEDOT sheets penetrate the gaps of the monofilaments, which may favor a highly conductive network and also increase the catalytic surface area of the CF/PEDOT CE.

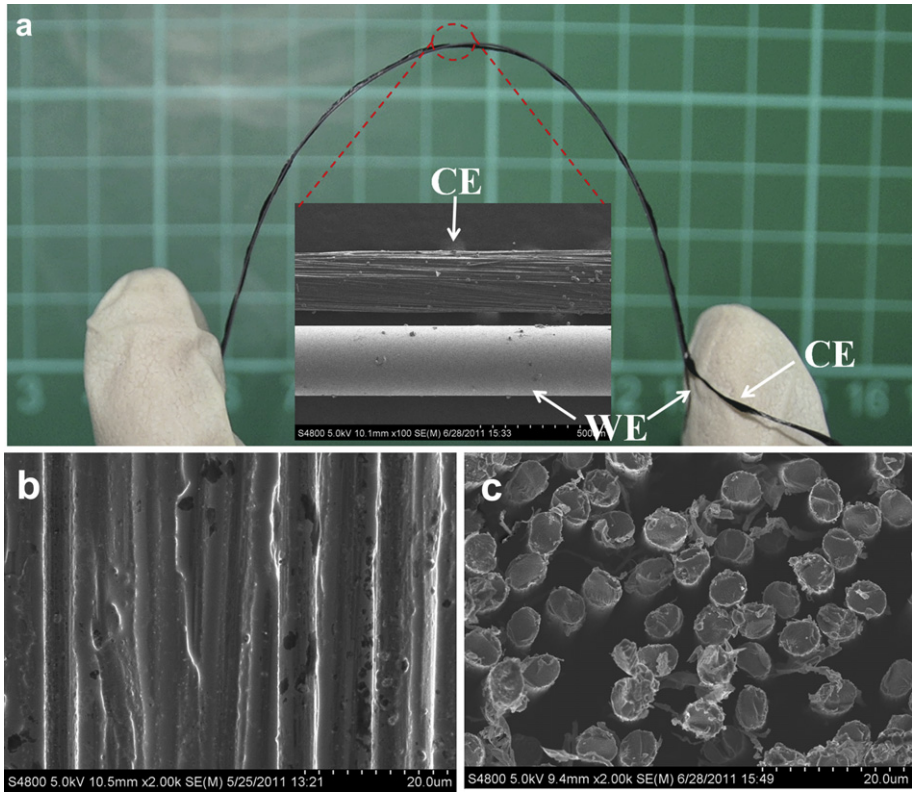

Fig. 1. a) Optical images of CF/PEDOT electrode (CE) and fiber photoanode (WE, *ca.* diameter of 270 μm and 70 mm length), the inset is an enlargement; b) SEM image of the CF/PEDOT CE; c) SEM image of the cross-section of the CF/PEDOT CE.

3.2. Electrochemical performance

CV was conducted to investigate the catalytic activity of the CF/PEDOT electrodes to I_3^-/I^- redox couples (Fig. 2). Fig. 2a shows the CV curves of the pure CF electrode (CF) and platinized CF electrode (CF/Pt), which was prepared *via* the thermal decomposition of chloroplatinic acid solution. As previously reported, from left to right, the two couples of the redox current peaks in the CV curves correspond to the I_3^-/I^- and I_3^-/I_2 redox reactions, respectively [36], and the left couple dominates the CE performance of the DSSCs. The reduction peak current of the pure CF was too small to be observed, showing its low catalytic performance. After modifying the CF with trace Pt, its reducing overpotential obviously decreased and its peak current dramatically increased, verifying the high catalytic activity of metallic Pt. The shape of the CV curve of the CF/PEDOT electrode was similar to that of the CF/Pt electrode, however, its left redox peak current was much larger. These results show that PEDOT has high catalytic activity. In addition, the current baseline of CF/PEDOT in the CV curve was higher than that of CF/Pt, probably because of the high charging current of the electric double layer at the PEDOT/electrolyte interface [28,29]. Fig. 2b shows 45 consecutive CV curves of CF/PEDOT and CF/Pt electrode. The left reduction peak potential of the CF/Pt shifted to the left, and the corresponding peak current decreased with increasing the cycle times. These results indicate that the catalytic activity of CF/Pt electrode weakens with increased cycle times, which is mainly caused by the surface adsorption of reduced species on Pt clusters that suppresses the catalytic reduction in the following steps [24]. Catalyst poisoning is detrimental to device performance, especially to the long term stability of DSSCs. The CV curves of the CF/PEDOT electrode in 45 continuous cycles were almost completely overlapping, with little changes in peak potential and current. The CF/PEDOT electrode showed a higher electrochemical stability than the CF/Pt electrode.

Fig. 2c shows the CV curves of CF/Pt and CF/PEDOT at different scanning rates, and the relationships of the left redox peak current and the square root of the scanning rates were also derived (Fig. 2d) to further investigate the dynamic electrochemical process of the CF-based electrodes. The linear relationships indicate that the diffusion process of redox species dominates the redox reactions [21,28,29]. The electrochemical results show that the CF/PEDOT electrode could probably be an alternative to CF/Pt electrode for efficient DSSCs.

3.3. Photovoltaic performance

The CF, CF/PEDOT, and CF/Pt CEs were combined with Ti wire-based photoanodes to fabricate fiber-shaped DSSCs, which were denoted as D_{CF}, $D_{CF-PEDOT}$, and D_{CF-Pt}, respectively. Fig. 3a shows the current–voltage (I–V) curves of the fiber-shaped DSSCs, and their photovoltaic parameters are summarized in Table 1. The open-circuit voltage (V_{oc}), short-circuit current (J_{sc}), fill factor (FF), and photoelectric conversion efficiency (PCE) of D_{CF} were 0.481 V, 7.49 mA cm^{-2}, 0.27, and 0.98%, respectively. The poor catalytic activity of the CF was the main cause of the poor photovoltaic performance of D_{CF}. The V_{oc}, J_{sc}, FF, and PCE of D_{CF-Pt} were raised to 0.685 V, 11.13 mA cm^{-2}, 0.67, and 5.08%, respectively, which are close to the best performance of fiber-shaped DSSCs based on CF/Pt CE prepared *via* sputtering [36]. Compared with D_{CF-Pt}, $D_{CF-PEDOT}$ had higher J_{sc} (12.01 mA cm^{-2}) and FF (0.69), and its PCE increased to 5.6%. The superior photovoltaic performance of $D_{CF-PEDOT}$ to D_{CF-Pt} demonstrates that the highly efficient CF/PEDOT electrode could replace the CF/Pt electrode.

The electrochemical impedances of the devices above were measured *in situ* to further explore the influence of CEs on device performance. Fig. 3b shows the Nyquist plots of D_{CF} and $D_{CF-PEDOT}$. The two arcs indicate the existence of two interfaces, that is,

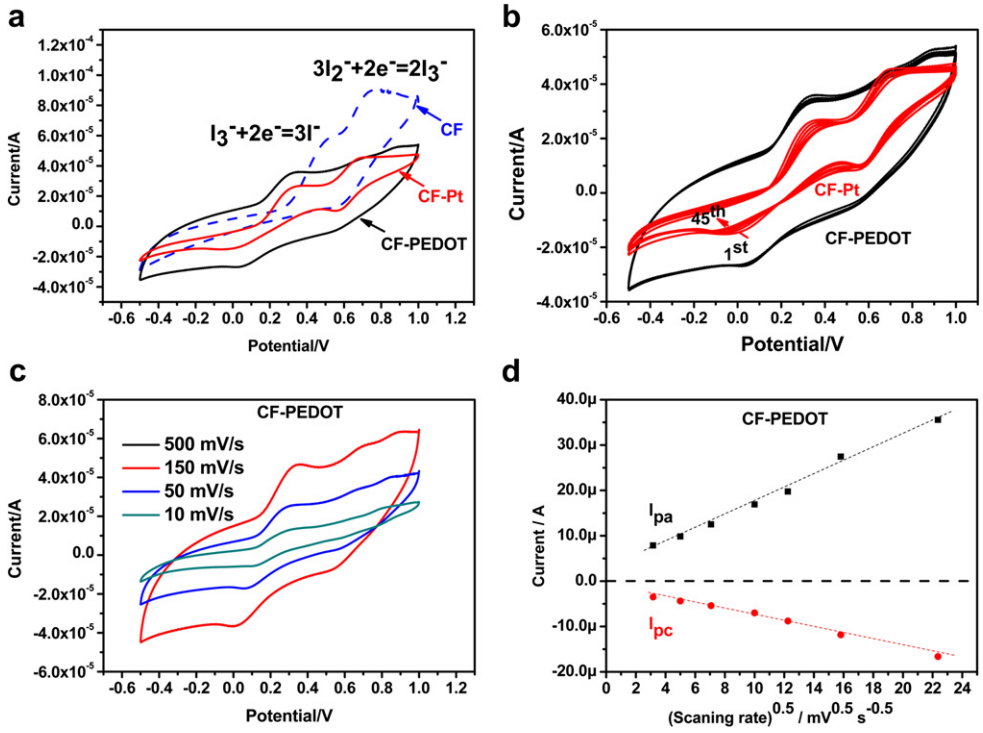

Fig. 2. a) CVs of the CF, CF/PEDOT, and CF/Pt CEs with a scan rate of 100 mV s^{-1}; b) Parts of the 45 consecutive CVs of CF/PEDOT and CF/Pt CEs with a scan rate of 100 mV s^{-1}; c) CVs of the CF–PEDOT electrode with different scan rates (from inner to outer: 10, 25, 50, 100, 150, 250, 350, and 500 mV s^{-1}, respectively); d) The relationship between the redox peak current and the scan rates of the CF/PEDOT electrode.

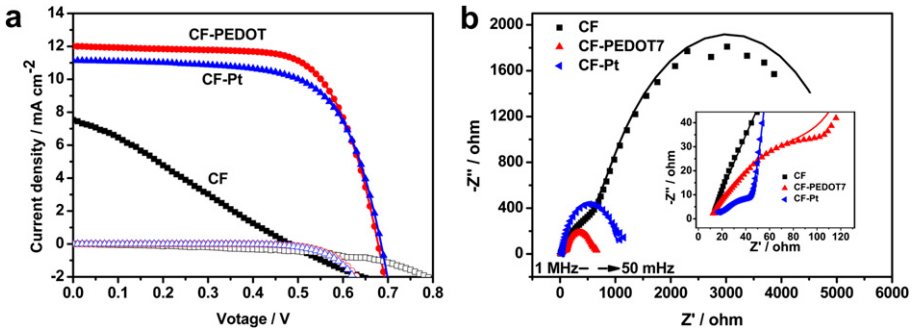

Fig. 3. a) Current density–Voltage curves of D_{CF}, $D_{CF-PEDOT}$, and D_{CF-Pt} under 100 mW cm^{-2} (AM 1.5G) simulated irradiation; b) Nyquist plots of D_{CF}, $D_{CF-PEDOT}$, and D_{CF-Pt}, namely the fiber-shaped DSSCs employing CF, CF/PEDOT, and CF/Pt CEs, respectively.

CE/electrolyte interface (high frequency region) and photoanode/electrolyte interface (low frequency region). The charge transfer resistance (R_{CT}) at the former interface and the series ohmic resistance (R_s), which have negative effects on device performance, were obtained *via* fitting with a simplified electric circuit model [36]. The R_s and R_{CT} changed with the conductivity and catalytic performance of the CEs because all the devices in the current study were prepared under the same conditions except with different CEs. The small R_s but large R_{CT} of D_{CF} were consistent with the good conductivity but poor catalytic performance of the CF electrode. The R_{CT} of $D_{CF-PEDOT}$ was reduced from 819.8 Ω to 137.6 Ω, while its R_s changed a little compared with that of D_{CF}, indicating that the CF substrate dominated the conductivity of the CF/PEDOT composite fiber. These results also prove that the PEDOT modification of CF could decrease the R_{CT} and lead to the catalytic CF/PEDOT CE. Moreover, the total series resistance was reduced, and the corresponding photovoltaic performance was dramatically improved.

Table 1
Photovoltaic parameters and EIS data of fiber-shaped DSSCs with different CEs.

Device	R_S [Ω]	R_{CT} [Ω]	V_{oc} [V]	FF	J_{sc} [mA cm^{-2}]	PCE [%]
D_{CF150}	11.1	819.8	0.481	0.27	7.49	0.98
$D_{CF150-PEDOT2}$	15.4	225.1	0.730	0.71	9.17	5.08
$D_{CF150-PEDOT4}$	12.3	208.2	0.685	0.70	11.15	4.73
$D_{CF150-PEDOT7}$	10.3	137.6	0.678	0.69	12.01	5.34
$D_{CF50-PEDOT4}$	41.1	259.1	0.723	0.64	8.58	5.61
$D_{CF100-PEDOT4}$	20.7	213.2	0.737	0.67	9.60	3.97

3.4. Optimization the amount of PEDOT and the diameters of CF/PEDOT electrodes

The influence of different PEDOT amount as well as the diameters of the CF/PEDOT electrodes were investigated to improve the device performance. During the experiment, the amount of PEDOT could easily be controlled *via* the number of applied dip-coatings. The performances of the devices using CF/PEDOT CEs with

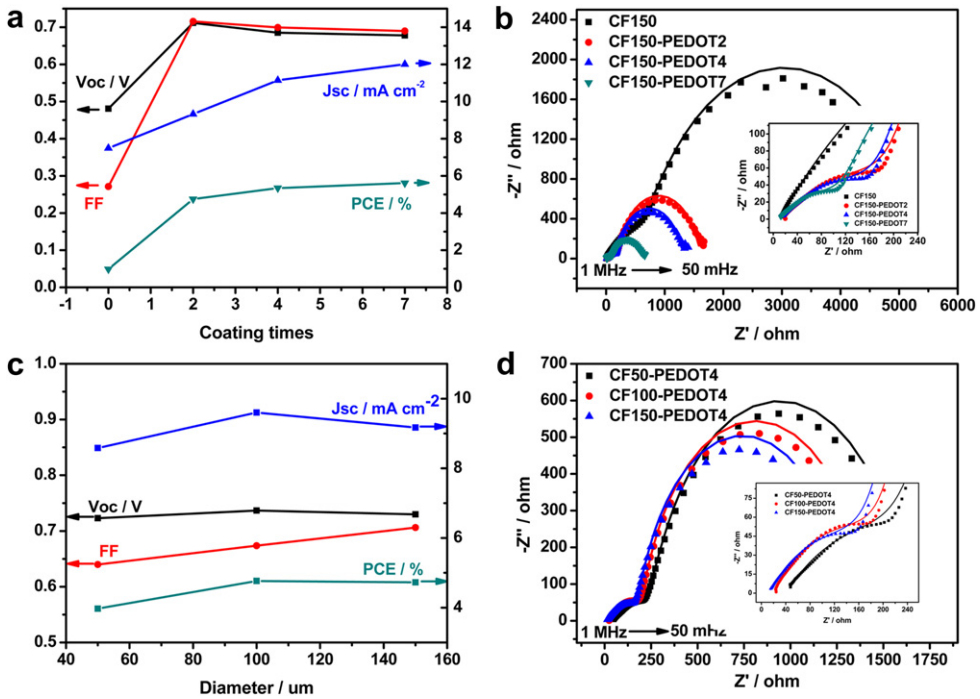

Fig. 4. a) The relationship between the photovoltaic parameters and the number of dip-coatings of D_{CF150}, $D_{CF150-PEDOT2}$, $D_{CF150-PEDOT4}$, and $D_{CF150-PEDOT7}$ (PEDOT dip-coating times: 0, 2, 4, and 7 times, respectively) under 100 mW cm^{-2} (AM 1.5G) simulated irradiation; b) Nyquist plots of these devices; c) The relationship between the photovoltaic parameters and the diameters of the CF/PEDOT CEs; d) Nyquist plots of $D_{CF50-PEDOT4}$, $D_{CF100-PEDOT4}$, and $D_{CF150-PEDOT4}$ (the diameters of CE were 50,100, and 150 μm, respectively).

different numbers of dip-coating applications (0, 2, 4, and 7) are summarized in Table 1. Fig. 4a shows that the photovoltaic parameters changed with number of applied coatings. After coating the CF with the PEDOT solution twice ($D_{CF150-PEDOT2}$), the V_{oc}, J_{sc}, FF, and PCE were 0.730 V, 9.17 mA cm^{-2}, 0.71, and 4.73%, respectively, suggesting that a small amount of PEDOT could significantly improve the photovoltaic performance. The parameters did not change apparently with the further increase in coating applications. PCE only increased to 5.6% even when it was coated with PEDOT seven times ($D_{CF150-PEDOT7}$). Moreover, electrochemical impedance spectroscopy (EIS) can explain these relationships. The R_{CT} of $D_{CF150-PEDOT2}$ in the Nyquist plots (Fig. 4b) dropped considerably to 225.1 Ω, and thus better device performance was achieved. However, the R_S and R_{CT} decreased slightly when the coating times were further increased, indicating a slight improvement in the conductivity and catalytic performance of the CF/PEDOT electrodes, which are in agreement with the device performance above.

Fig. 4c and d demonstrates the photovoltaic performance and EIS results of the fiber-shaped DSSCs using CF/PEDOT CEs with diameters of 50, 100 and 150 μm, respectively. The J_{sc} and V_{oc} slightly changed, while the FF increased from 0.64 to 0.67 and the PCE increased from 3.97% to 4.77% when the diameter of the CF/PEDOT increased from 50 μm to 150 μm, as shown in Fig. 4c. These changes illustrate that the diameter of the CF/PEDOT CE had weaker effects on device performance than the number of dip-coatings. The EIS confirmed that the R_S dropped by 50%, however, the R_{CT} dropped by only 17% when the diameter increased from 50 μm to 150 μm. The decrease in R_S can be attributed to the improvement in the conductivity of the CF/PEDOT CE with large diameters because more CF monofilaments provide more conductive paths. However, the CF/PEDOT electrodes with large diameters were too thick for the redox species to diffuse in or out. Therefore, the effective catalytic surface and resulting photovoltaic performance minimally improved. Moreover, assembling a device CE with too thick a coating of PEDOT on CFs is not easy. Thus, the CF/PEDOT CEs with diameters of 150 μm were used to fabricate fiber-shaped DSSCs.

Fiber-shaped DSSCs using flexible and metal-free CF/PEDOT electrodes as CEs work better than those using CF/Pt CEs under different light density (Figure S1a). Moreover, these fiber-shaped DSSCs show low dependence on the light incident angle because of their highly symmetrical device structure and unique 3D optical structure (Figure S1b). The power output could also be greatly enhanced by simply placing a light diffusion board under the device (Figure S1c).

4. Conclusion

Highly conductive and catalytic CF/PEDOT electrodes with multiple core/shell structures were prepared using commercially available materials and a simple method. Moreover, the optimization of the amount of PEDOT and the diameters of the CF/PEDOT CEs led to highly efficient fiber-shaped DSSCs with a highest efficiency of 5.5%. The biocompatible CF/PEDOT composite electrodes have the advantages of low cost, light weight, and high flexibility. Therefore, they are preferable to using metal electrodes. These results also indicate a good prospect of their applications in fiber/wearable electronics.

Acknowledgments

This work was jointly supported by MOST (2011CB933300), NSFC (50833001), and MOE (309001), China.

Appendix A. Supplementary material

Supplementary material associated with this article can be found, in the online version, at doi:10.1016/j.jpowsour.2012.05.002.

References

[1] B. Oregan, M. Gratzel, Nature 353 (1991) 737–740.
[2] N. Papageorgiou, Coord. Chem. Rev. 248 (2004) 1421–1446.

[3] T.N. Murakami, M. Gratzel, Inorg. Chim. Acta 361 (2008) 572–580.
[4] A. Kay, M. Gratzel, Sol. Energy Mater Sol. Cells 44 (1996) 99–117.
[5] T.N. Murakami, S. Ito, Q. Wang, M.K. Nazeeruddin, T. Bessho, I. Cesar, P. Liska, R. Humphry-Baker, P. Comte, P. Pechy, M. Gratzel, J. Electrochem. Soc. 153 (2006) A2255–A2261.
[6] S.Q. Fan, B. Fang, J.H. Kim, B. Jeong, C. Kim, J.S. Yu, J. Ko, Langmuir 26 (2010) 13644–13649.
[7] P. Joshi, L.F. Zhang, Q.L. Chen, D. Galipeau, H. Fong, Q.Q. Qiao, ACS Appl. Mater. Interfaces 2 (2010) 3572–3577.
[8] B.K. Koo, D.Y. Lee, H.J. Kim, W.J. Lee, J.S. Song, H.J. Kim, J. Electroceram. 17 (2006) 79–82.
[9] J.D. Roy-Mayhew, D.J. Bozym, C. Punckt, I.A. Aksay, ACS Nano 4 (2010) 6203–6211.
[10] J.H.Y. Ladislav Kavan, Michael Gratzel, ACS Nano 5 (2010) 165–172.
[11] S.H. Seo, S.Y. Kim, B.K. Koo, S.I. Cha, D.Y. Lee, Langmuir 26 (2010) 10341–10346.
[12] Q.W. Jiang, G.R. Li, X.P. Gao, Chem. Commun. 44 (2009) 6720–6722.
[13] J.S. Jang, D.J. Ham, E. Ramasamy, J. Lee, J.S. Lee, Chem. Commun. 46 (2010) 8600–8602.
[14] S.M. Zakeeruddin, M.K. Wang, A.M. Anghel, B. Marsan, N.L.C. Ha, N. Pootrakulchote, M. Gratzel, J. Am. Chem. Soc. 131 (2009) 15976–15977.
[15] M.X. Wu, X.A. Lin, A. Hagfeldt, T.L. Ma, Chem. Commun. 47 (2011) 4535–4537.
[16] Q.H. Li, J.H. Wu, Q.W. Tang, Z. Lan, P.J. Li, J.M. Lin, L.Q. Fan, Electrochem. Commun. 10 (2008) 1299–1302.
[17] Z.P. Li, B.X. Ye, X.D. Hu, X.Y. Ma, X.P. Zhang, Y.Q. Deng, Electrochem. Commun. 11 (2009) 1768–1771.
[18] J. Zhang, T. Hreid, X.X. Li, W. Guo, L.P. Wang, X.T. Shi, H.Q. Su, Z.B. Yuan, Electrochim. Acta 55 (2010) 3664–3668.
[19] S.S. Jeon, C. Kim, J. Ko, S.S. Im, J. Mater. Chem. 21 (2011) 8146–8151.
[20] J.B. Xia, L. Chen, S. Yanagida, J. Mater. Chem 21 (2011) 4644–4649.
[21] Y. Saito, W. Kubo, T. Kitamura, Y. Wada, S. Yanagida, J. Photochem. Photobiol. A 164 (2004) 153–157.
[22] S. Yanagida, J.B. Xia, N. Masaki, K.J. Jiang, J. Mater. Chem. 17 (2007) 2845–2850.
[23] J.M. Pringle, V. Armel, D.R. MacFarlane, Chem. Commun. 46 (2010) 5367–5369.
[24] H.N. Tian, Z. Yu, A. Hagfeldt, L. Kloo, L. Sun, J. Am. Chem. Soc. 133 (2011) 9413–9422.
[25] G.Q. Shi, W.J. Hong, Y.X. Xu, G.W. Lu, C. Li, Electrochem. Commun. 10 (2008) 1555–1558.
[26] K. Kitamura, S. Shiratori, Nanotechnology 22 (2011) 195703–195708.
[27] J. Zhang, X.X. Li, W. Guo, T. Hreid, J.F. Hou, H.Q. Su, Z.B. Yuan, Electrochim. Acta 56 (2011) 3147–3152.
[28] K. Kobayashi, S. Sakurai, H.Q. Jiang, M. Takahashi, Electrochim. Acta 54 (2009) 5463–5469.
[29] M.H. Yeh, L.Y. Lin, C.P. Lee, H.Y. Wei, Ch. Y. Chen, Ch. G. Wu, R. Vittal, K.Ch. Ho, J. Mater. Chem. 21 (2011) 19021–19029.
[30] X. Fan, Z.Z. Chu, F.Z. Wang, C. Zhang, L. Chen, Y.W. Tang, D.C. Zou, Adv. Mater. 20 (2008) 592–595.
[31] M.R. Lee, R.D. Eckert, K. Forberich, G. Dennler, C.J. Brabec, R.A. Gaudiana, Science 324 (2009) 232–235.
[32] Z.Y. Liu, M. Misra, ACS Nano 4 (2010) 2196–2200.
[33] Z. Lv, Y. Fu, S. Hou, D. Wang, H. Wu, C. Zhang, Z. Chu, D. Zou, Phys. Chem. Chem. Phys. 13 (2011) 10076–10083.
[34] D. Wang, S. Hou, H. Wu, C. Zhang, Z. Chu, D. Zou, J. Mater. Chem. 21 (2011) 6383–6388.
[35] Y. Fu, Z. Lv, S. Hou, H. Wu, D. Wang, C. Zhang, Z. Chu, X. Cai, X. Fan, Z.L. Wang, D. Zou, Energy Environ. Sci. 4 (2011) 3379–3383.
[36] S. Hou, X. Cai, Y. Fu, Z. Lv, D. Wang, H. Wu, C. Zhang, Z. Chu, D. Zou, J. Mater. Chem. 21 (2011) 13776–13779.
[37] J.G. Chen, H.Y. Wei, K.C. Ho, Sol. Energy Mater Sol. Cells 9 (2007) 1472–1477.